Available online at www.sciencedirect.com

SciVerse ScienceDirect

Ceramics International 39 (2013) 2323–2330

CERAMICS INTERNATIONAL

www.elsevier.com/locate/ceramint

ZnO–Ag ceramics for ethanol sensors

A.Yu. Lyashkov[a,*], A.S. Tonkoshkur[a], J.A. Aguilar-Martinez[b], A.B. Glot[c]

[a]Dniepropetrovsk National University, Gagarin av. 72, Dniepropetrovsk 49010, Ukraine
[b]Centro de Investigación en Materiales Avanzados, S.C. (CIMAV), Alianza Norte No. 202, Parque de Investigación e Innovación Tecnológica (PIIT), Nueva carr. Aeropuerto km. 10 C.P. Apodaca N.L. 66600, México
[c]Universidad Tecnológica de la Mixteca, Huajuapan de León, Oaxaca 69000, México

Received 25 June 2012; received in revised form 14 August 2012; accepted 28 August 2012
Available online 4 September 2012

Abstract

The structure and electrical properties of the ZnO–Ag (0.001–3 wt%) ceramics in air and in air with the ethanol addition are studied. It was found that electrical parameters are sensitive to the concentration of ethanol in air due to a decrease in the barrier height at the grain boundaries. Silver addition causes a decrease in the density of material due to the formation of Ag inclusions. This can be the main reason of higher sensitivity to ethanol observed in ZnO–Ag ceramics in comparison with other ZnO–based ceramics.

Keywords: E. Sensor; Ethanol sensor; Grain boundary; ZnO-based ceramics

1. Introduction

Zinc oxide with different additives is frequently used for the preparation of gas sensors [1,2]. The details of the preparation and structure have a strong influence on the physico-chemical processes related to their gas sensitivity [3–5]. Several catalytically active metals like Pt [6,7], Pd [8–10], Au [11,12], Ag [13,14] can be used for the improvement of the sensitivity and selectivity of the ZnO-based sensors.

The ZnO ceramics with Ag addition exhibit relatively high sensitivity to the alcohol vapors and, therefore, they are considered as the most prospective sensor materials for this group of gases [14]. The optimization of the production technology of these materials needs the detailed data about the structure, the electro-physical properties and the mechanisms of their gas sensitivity. To date, however, proper attention to such investigations was not given probably due to some general difficulties in realization of the heterogeneous experiments and in the interpretation of the electro-physical processes in disordered materials. A few works on ZnO–Ag materials were devoted mainly to the study of their structure and optical properties [15–28].

With the aim to understand the role of Ag addition, in this paper the microstructure, the electrical properties in air and the ethanol-sensing behavior of the ZnO–Ag ceramics with different amount of Ag_2O addition are studied and discussed.

2. Experimental details

2.1. Samples

The ZnO ceramics were prepared by the conventional oxide mixture method. The ZnO and Ag_2O powders of submicron size were mixed using ethyl alcohol and then dried. The amount of Ag_2O addition was varied in the range 0.001–3 wt%. The obtained powder was pressed in tablets of 12 mm in diameter and up to 4 mm in thickness under the axial pressure of 100 MPa.

The sintering of ZnO–Ag_2O was performed during 1 h at temperature 1170 K which is below the melting temperature of silver. The independent repetition of the sintering of samples with different amount of Ag_2O addition gave reproducible parameters. For the electrical measurements Ag electrodes at the same plane surface or at the opposite plane surfaces were obtained. Additionally, ZnO–Ag_2O, ZnO–CoO, ZnO–CuO (0.5 at% of added metal) and pure

*Corresponding author.
E-mail address: vdnu@narod.ru (A.Yu. Lyashkov).

0272-8842/$ - see front matter © 2012 Elsevier Ltd and Techna Group S.r.l. All rights reserved.
http://dx.doi.org/10.1016/j.ceramint.2012.08.080

ZnO ceramics were sintered simultaneously in the furnace with a low temperature gradient at slightly higher temperature 1270 K to ensure the doping of ZnO crystallites.

2.2. Microstructure and phase composition

The scanning electron microscopy (SEM) of the surface and the energy-dispersive X-ray (EDX) microanalysis were performed in the microscopes Nova NanoSEM 200 (FEI Company, USA) and REM-106I (SELMI, Ukraine). The X-ray diffraction (XRD) was studied in the filtered CuK_α ($\lambda = 1.5406$ Å) emission using the diffractometer PANalytical Empyrean. The phases were identified using X'Pert Highscore plus and ICDD PDF-2 data.

The linear shrinkage γ was calculated according to the expression: $\gamma = (d_o - d)/d_o$, where d_o and d are the diameters of a sample before and after the sintering, respectively. The density ρ of the sintered samples was calculated according to the expression $\rho = m/V$, where m is the mass found from the weighting of a sample in air and V is the volume of a sample. The relative density was defined as ρ/ρ_0, where ρ_0 is the theoretical density. For ZnO–Ag the theoretical density was calculated taking into account the chemical composition before the sintering. For pure ZnO the value $\rho_o = 5.66\ \mathrm{g\ cm^{-3}}$ was used.

2.3. Electrical measurements

The dc current–voltage characteristics and the temperature dependence of the dc low-field electrical conductivity $\sigma(T)$ were obtained in air using commercial digital devices. The nonlinearity coefficient $\beta = (E/j)(dj/dE)$ was estimated according to the expression $\beta = \log(J_2/J_1)/\log(E_2/E_1)$, where $J_1 = 0.4\ \mathrm{mA\ cm^{-2}}$ and $J_2 = 4\ \mathrm{mA\ cm^{-2}}$are the current densities, E_1 and E_2 are respective values of the electric field. The $\sigma(T)$ dependence was obtained at heating and cooling of a sample with a rate of about 1.5 K/min. The activation energy of electrical conduction E_σ was found from the equation $\sigma(T) = \sigma_0 \exp(-E_\sigma/kT)$, where $\sigma(T)$ is the electrical conductivity at the absolute temperature T, σ_0 is a constant, k is Boltzmann's constant. The frequency dependence of the relative dielectric permittivity ε' and the coefficient of dielectric losses ε'' were recorded in air using the unit BM-560. The dc losses were not subtracted due to they were relatively low (not more than 1%).

The sensor properties were studied in the chamber of about $2 \cdot 10^4\ \mathrm{cm^3}$ with air atmosphere. Some necessary amount of liquid alcohol was put inside. After the evaporation of this liquid, the necessary partial pressure of ethanol in air was established. The temperature of the sample was measured using the chromel–copel thermocouple. For the recovery after each experiment a sample was heated at T ~ 720 K during 30 min. The response was calculated as $(\sigma - \sigma_0)/\sigma_0$, where σ is the conductance of a sample in air with ethanol and σ_0 is the conductance in air without gas. The kinetics of the response was studied by the introducing/withdrawing of a sensor to/from the measurement chamber. The response time $t_{0.9}$ was defined as the time interval for the signal to be changed between 10 and 90% of the signal amplitude (value $\sigma - \sigma_0$). The recovery time $t_{0.1}$was defined as the time interval for the signal to be decreased to the level of 10% higher than σ_0. The dependence of the response on the partial pressure of ethanol in air was obtained using the kinetic data. The temperature dependence of the response was measured at heating of a sample with a rate of 5 K/min.

2.4. Results processing

The degree of connection between different experimental values was estimated using the coefficient of determination $R^2(a,b)$ (the coefficient of linear correlation $R(a,b)$squared) [29]:

$$R(a,b) = \frac{\sum_{i=1}^{n} (a_i - \overline{a})(b_i - \overline{b})}{s_a s_b (n-1)} \quad (1)$$

where a_i and b_i are random quantities, $\overline{a}$ and $\overline{b}$ are the average values of these parameters defined as $\overline{a} = n^{-1} \sum_{i=1}^{n} a_i$. The root-mean-square deviation s_a and s_b are defined by the expression

$$s_a = \sqrt{(n-1)^{-1} \sum_{i=1}^{n} (a_i - \overline{a})^2} \quad (2)$$

where i is the current number of the sampling unit, n is the number of elements in the sampling.

3. Experimental results and discussion

3.1. Structure and electro-physical properties

The X-ray diffraction data indicate the presence only the crystalline ZnO and the metallic Ag phase (Fig. 1). Before the sintering the amount of Ag_2O was 3 wt%. After the sintering the amount of metallic Ag was 2.0 wt%. Therefore, it is assumed that the reduction of silver takes place at high temperature. This fact can be due to the partial evaporation of Ag during sintering. Below some confirmation of this suggestion is mentioned. Thus, obtained ceramic material is the ZnO–Ag semiconductor-metal composite.

The ZnO–Ag ceramics exhibit slightly rose bloom. In the optical microscope at the as-sintered surface of the sample the dark clusters with the characteristic metallic luster are seen. This probably can be explained by the partial reduction of Ag at the sintering and subsequent oxidation of Ag at cooling. The largest Ag inclusions are rather less than 1–2 μm. The semiconductor phase of the obtained ZnO–Ag composite is polycrystalline with the grain size D of ZnO grains in the range 0.3–0.4 μm depending on the amount of Ag_2O addition (Table 1).

The silver inclusions (clusters) were not detected by SEM/EDX at the as-sintered surface. But the silver inclusions with

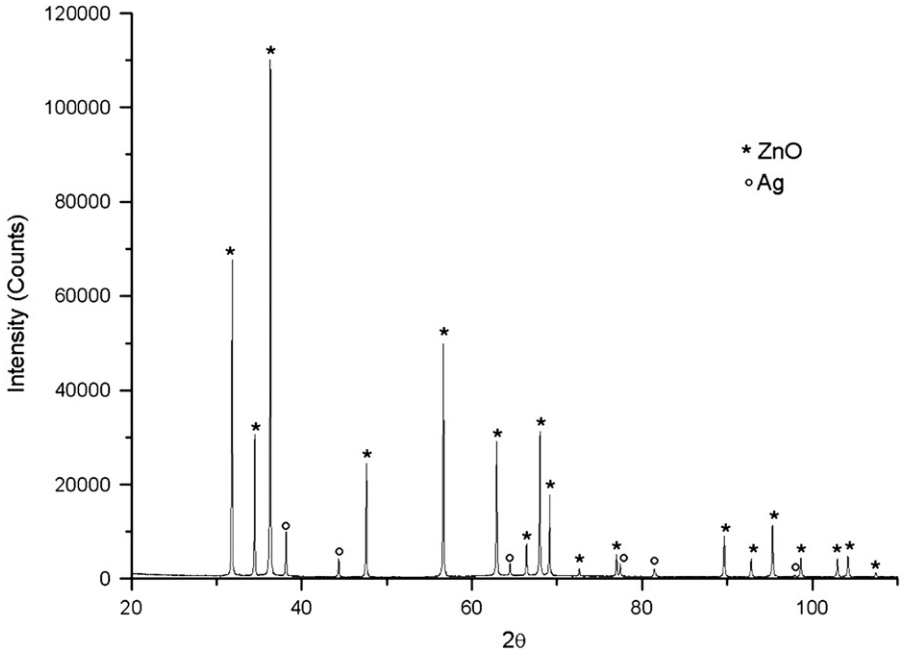

Fig. 1. XRD pattern for the sample ZnO-3 wt%Ag_2O (✻—ZnO; *o*—Ag).

Table 1
Some parameters of ZnO–Ag ceramics.

Ag_2O addition m_d (wt%)	Linear shrinkage γ (%)	Relative density ρ/ρ_0	Grain size D (μm)	Electrical conductivity (at 10 V cm^{-1}) σ_0, (Ohm^{-1} cm^{-1})
0	17.6	0.79	0.38	1.3×10^{-7}
0.001	13.7	0.74	0.39	1.3×10^{-8}
0.01	13.0	0.7	0.40	2.2×10^{-8}
0.1	11.6	0.7	0.35	1.7×10^{-8}
0.5	12.2	0.61	0.34	8.9×10^{-10}
1	13.7	0.66	0.40	4.7×10^{-9}
1.5	9.8	0.47	0.38	1.4×10^{-9}
2	11.3	0.62	0.35	8.6×10^{-9}
3	6.7	0.49	0.29	2.7×10^{-9}

the size 0.2–1.5 μm were observed after the grinding of some thin layer (Fig. 2a and b). This can be due to more intensive evaporation of Ag from the surface regions during the sintering. Therefore, the Ag inclusions are more typical for the inner regions of this material. This result is in according to the optical microscopy and the XRD data.

The linear shrinkage γ, the relative density ρ/ρ_0 and the low-field electrical conductivity σ are decreased with Ag_2O addition though some scattering takes place (Table 1). The reason for this fact can be related to the random formation of pores in this material. With the aim to prove that there is a correlation between these parameters, the statistical analysis was applied (see Section 2.4). It was found that between the amount of added Ag (m_d) and the relative density ρ/ρ_0) exists so called "strong connection" [29] because $R^2(m_d,\rho/\rho_0)=0.65$. Also the "strong connection" was observed between the electrical conductivity and the relative density ($R^2(\log\sigma,\rho/\rho_0)=0.68$). Therefore, the increase in amount of the Ag addition leads to the decrease in the density and the electrical conductivity. The inclusions of Ag do not form a liquid phase and do not solve the main substance (ZnO). Therefore, such Ag inclusions impede the mass transfer and the movement of the grain boundaries. As a result, the material becomes more porous and exhibit lower relative density. The similar situation takes place in other materials [30].

The current–voltage characteristics of ZnO–Ag ceramics are nonlinear but the nonlinearity coefficient is quite low. The increase in Ag addition causes the shift of the current–voltage characteristics to the high-field region and decrease in the nonlinearity coefficient from 2.6 for pure ZnO to 2.0 for ZnO with 3 wt% of Ag_2O (Fig. 3).

The frequency dependences of the relative dielectric permittivity $\varepsilon'(f)$ and the coefficient of dielectric losses $\varepsilon''(f)$ exhibit dispersion in the range of radio frequencies (Fig. 4). This dispersion is usually related to the Maxwell–Wagner–Sillars displacement of free electrons in the conductive phase of the inhomogeneous material (ZnO crystallites) [31]. As it is seen,

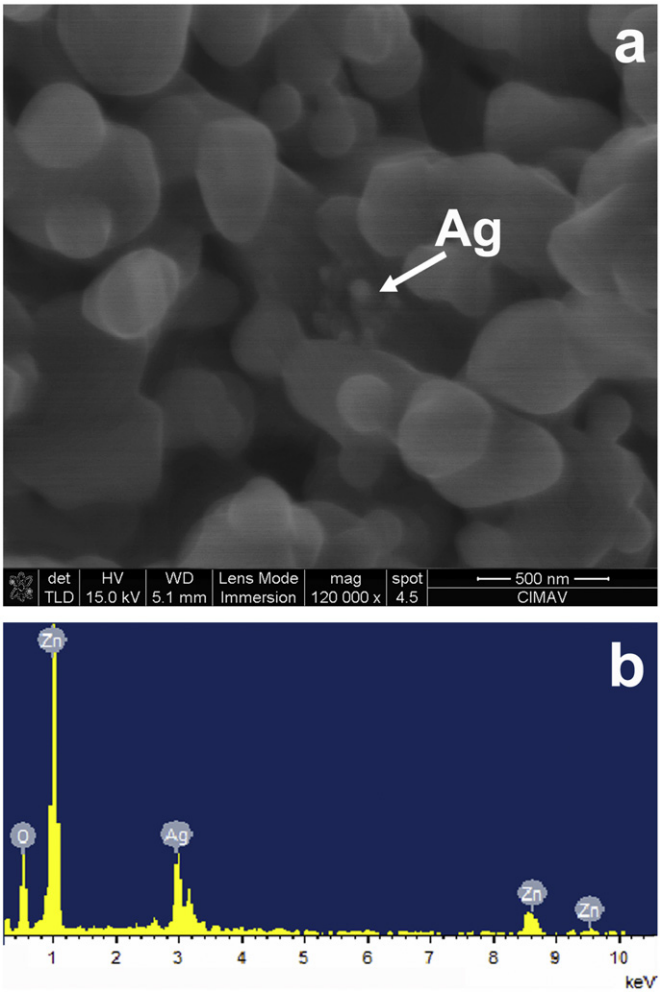

Fig. 2. (a) Secondary electron image and (b) energy-dispersive X-ray spectrum obtained after the grinding of thin layer. Sample ZnO-3 wt% Ag_2O.

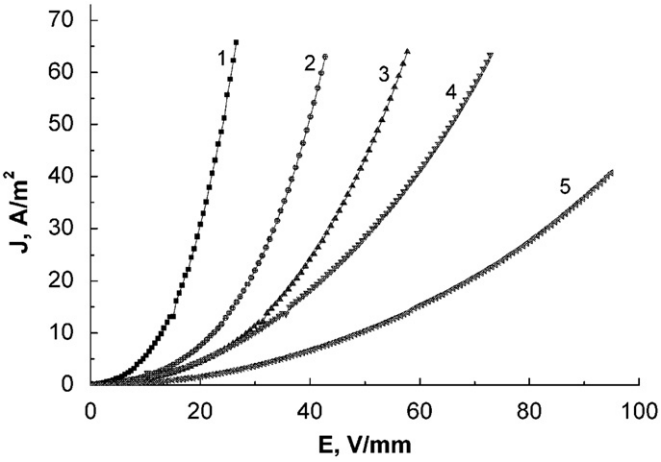

Fig. 3. Current–voltage characteristics (in air) of ZnO–Ag ceramics with different Ag_2O addition (wt%): 1–0; 2–0,01; 3–0,1; 4–1 and 5–2.

at increase in Ag_2O addition the shift of this dispersion to lower frequencies is observed. In the frames of the Maxwell–Wagner–Sillars polarization model it means the decrease in the electrical conductivity of ZnO crystallites.

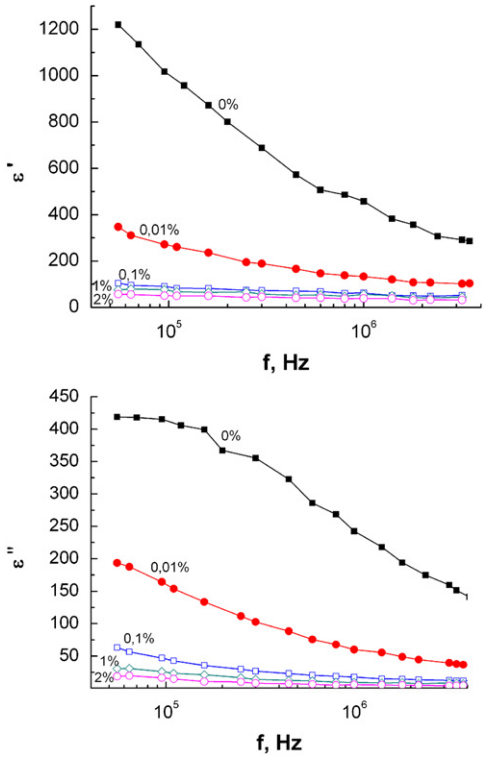

Fig. 4. Dependences of relative dielectric permittivity ε' and coefficient of dielectric losses ε'' on frequency in ZnO–Ag ceramics with different Ag_2O additions (wt%).

Taking into account that in the polycrystalline ZnO the potential barriers at the grain boundaries can be formed [32], the observed effects can be explained in terms of the grain-boundary potential barriers formed in the ZnO–Ag ceramics. The activation energy of electrical conduction $E_\sigma = 0.2$–0.25 eV in the ZnO–Ag ceramics in air in the range 290–360 K can be approximately equal to the barrier height φ. The barrier height is slightly increased with the increase in Ag_2O addition. The appearance of the barriers at the interfaces between the ZnO grains and the Ag inclusions looks less probable due to the values of the work function (~4.2 eV) for both substances are close [33].

The atoms of silver in can create the acceptor levels situated about 0.2 eV above the valence band edge of ZnO [34]. Taking into consideration this information, it can be assumed that the observed shift of the current–voltage characteristics to the high-field region and the dielectric dispersion region to the lower frequencies with the increase in Ag_2O addition, can be explained by the decrease in the density of free electrons in ZnO grains due to the Ag doping.

3.2. Gas-sensitive properties

3.2.1. Influence of water vapor on electrical conductance

For the sensor of some gas in air it is very important to have a weak response to the water vapor in air because the water vapor is frequently presented in the ambient atmosphere. Usually H_2O adsorbed at the ZnO surface at room

temperature exhibit donor properties [35] and the resistance of a sample is decreased. The increase in the relative humidity w (partial pressure P_v of H_2O in air) indeed causes a decrease in the dc resistance, however, above about $w=40\%$ the resistance of the sensor is practically unchangeable.

The increase in temperature up to 340–360 K leads to the desorption of H_2O molecules and the response $(\sigma-\sigma_0)/\sigma_0$ is decreased (here σ is the conductance of a sample in humid air and σ_0 is the conductance in dry air). Therefore, the most strong influence of the water vapor on the electrical conductivity of ZnO–Ag ceramics takes place in the narrow temperature range near room temperature.

The activation energy of electrical conduction E_σ near room temperature found from $\sigma(T)$ dependence in humid air (the electrical conductance is increased with the decreasing temperature due to the adsorption of water molecules) is in the range 1.4–3.2 eV for different samples. This value can have the sense of the activation energy of water desorption [36]. Some minor growth of the electrical conductance at $T>500$ K with the activation energy 0.4–0.65 eV can be explained by the participation of H^+ ions in the conduction process. Therefore, the range 350–550 K could be acceptable operating temperature range for the sensor of ethanol in air because in this range its sensitivity to water vapor is very low.

3.2.2. Sensitivity to ethanol vapor in air

In Fig. 5 the dependence of the response $(\sigma-\sigma_0)/\sigma_0$ on the partial pressure P_a of ethanol in air is shown. The response values were measured at 600 s after the change of the gas media. It is seen from Fig. 5 that the pressure dependence of the response is approximated by the equation similar to the Freundlich isotherm $(\sigma-\sigma_0)\sigma_0^{-1}=A\,P_a^{\chi}$, where A and χ are constants [37].

The temperature dependences of the response have a maximum at 570–600 K and at higher partial pressures of ethanol the response is increased (Fig. 6). This maximum probably can be due to the competition of two general opposite factors: at increase of temperature the interaction of the surface with the gas ambient becomes more intensive and the response $(\sigma-\sigma_0)/\sigma_0$ is increased, however, at

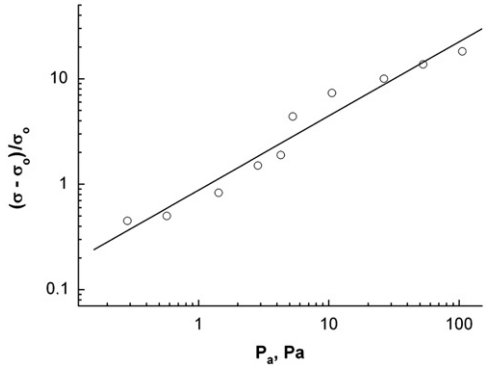

Fig. 5. Dependence of the response on partial pressure of ethanol in air at temperature 650 K at fixed time 600 s. Sample ZnO-2 wt% Ag_2O.

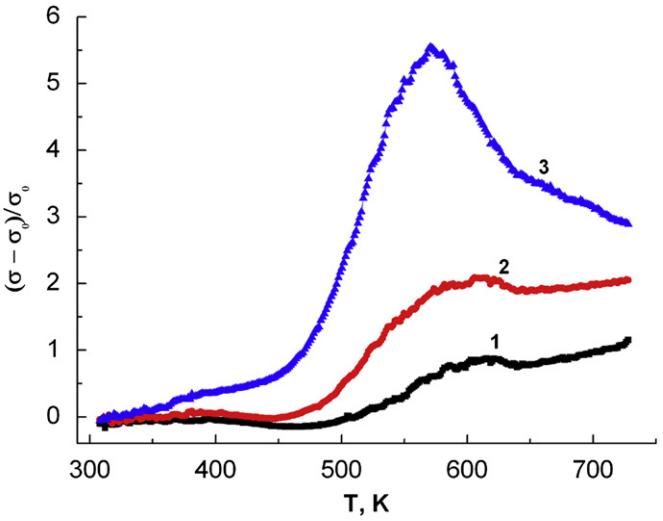

Fig. 6. Temperature dependence of response in air with different partial pressure of ethanol: 12 Pa (1); 24 Pa (2) and 136 Pa (3). Sample ZnO-0.01 wt% Ag_2O.

higher temperatures the conductance of material σ_0 is increased and the response $(\sigma-\sigma_0)/\sigma_0=(\sigma/\sigma_0)-1$ is decreased too.

The dependences of the response on the amount of Ag_2O addition m_d and the density ρ of ZnO–Ag ceramic material are shown in Fig. 7. It is seen from Fig. 6 that the response is linearly increased on logarithm of the amount of Ag_2O addition m_d (the coefficient of determination is $R^2((\sigma-\sigma_0)/\sigma_0,\ \log m_d)\approx 0.65$) and is decreased on the density ρ of a sample ($R^2((\sigma-\sigma_0)/\sigma_0,\ \rho)\approx 0.55$). Taking into account that the values m_d and ρ are correlated ($R^2\ (\rho,\ m_d)=0.65$, see Table 1) it can be assumed that the observed increase in the response on Ag_2O addition accompanied by the decrease in the density of a sample, is attributed to the increase in the specific surface of the ceramics.

3.3. Properties of ZnO ceramics with different additives

The ZnO ceramics without additives and with the addition of CoO, CuO, Ag_2O prepared at sintering temperature 1270 K, exhibit similar polycrystalline morphology with the grain size of about 1 μm. Some parameters of these ceramics are presented in Table 2.

The observed increase in the relative dielectric permittivity ε' and the coefficient of dielectric losses ε'' in ZnO–CoO ceramics can be explained by the shift of the dielectric dispersion region to higher frequencies due to the increase in the electrical conductivity of ZnO grains [31]. It can be a consequence of the increase in the free electron density in ZnO grains doped by the donor impurity (Co) [38].

Using the acceptor impurities Cu and Ag leads to a decrease in the density of electrons in ZnO grains and, respectively, to a decrease in the electrical conductivity of ZnO grains [34]. Therefore, the mentioned dielectric dispersion is displaced to lower frequencies. As a result, the relative dielectric permittivity ε' and the coefficient of dielectric losses

ε'' in ZnO–CuO and ZnO–Ag ceramics at fixed frequency (10^5 Hz) are decreased (Table 2).

It is necessary to mention that ionic radius of Ag^+ (0.113 nm) is higher than of Zn^{2+} (0.083 nm). This makes difficult the appearance of Ag in the interstitials. Some mechanical strains can occur in the crystalline lattice of ZnO grains in ZnO–Ag ceramics as it takes place in the ZnO–Ag thin films [34]. In the ZnO grains in ZnO–CuO ceramics probably such mechanical strains can be lower due to the lower ionic radius of Cu^+ (0.098 nm) and Cu^{2+} (0.080 nm). Therefore, some higher doping level of ZnO grains in ZnO–CuO ceramics than in ZnO–Ag ceramics (at other equal conditions) is expected.

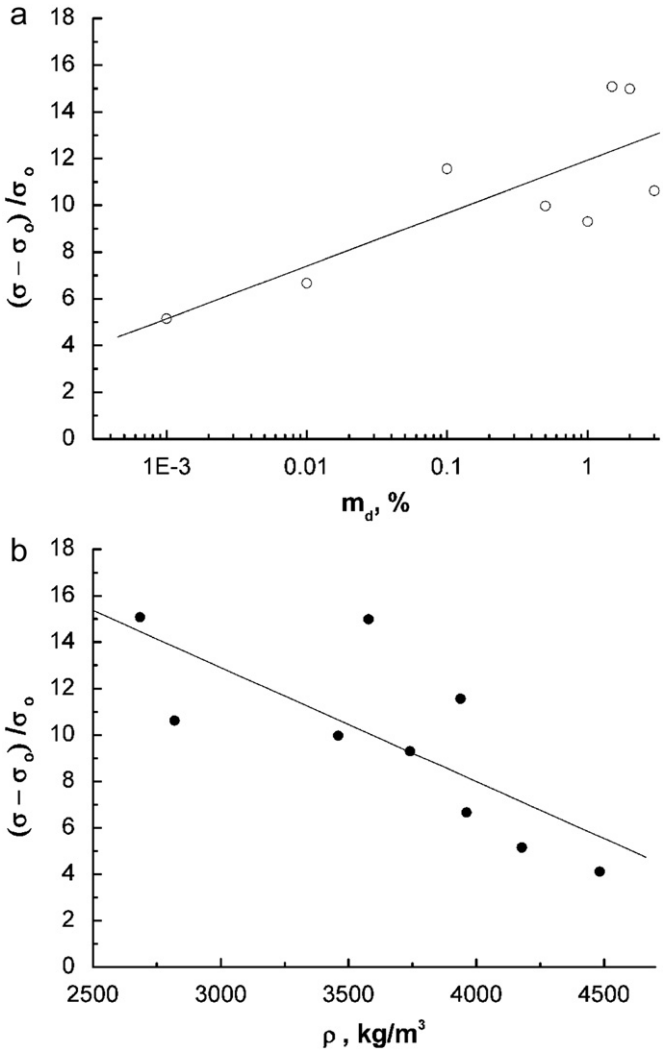

Fig. 7. Dependences of the response of ZnO–Ag ceramics (in air with partial pressure of ethanol $P_a=55$ Pa at fixed time 300 s) on the amount of Ag_2O addition m_d (a) and the density ρ (b). $T=650$ K.

From the view-point of the electron theory of catalysis [39] and the barrier mechanism of gas sensitivity [40] it can be assumed that the decrease in the free electron bulk density would lead to the decrease in the concentration of chemisorbed oxygen at the semiconductor surface and to the decrease in the response. This takes place in the case of the ZnO–CuO ceramics (Table 2). In the case of the ZnO–CoO ceramics the response is similar to the response for pure ZnO (Table 2). This fact can be explained by the complete filling of the surface by the adsorbed oxygen even in the undoped material due to the substantial concentration of the native defects [32]. Therefore, the doping by Co does not lead to an increase in the oxygen covering and the response (Table 2). The doping of ZnO by Ag_2O probably decreases the electrical conductivity of grains not as strongly as in the case of CuO. However, the response in the case of ZnO–Ag ceramics is significantly higher than for the ZnO ceramics with other additives prepared at the same conditions (Table 2). It can be due mainly to the quite low density (Table 2) and the developed surface in the ZnO–Ag ceramics. Probably silver inclusions at the initial stages of the sintering create obstacles for the movement of the grain boundaries. As a result the porous material with small grains is formed. This assumption is confirmed by the fact that the increase in the sintering temperature leads to the increase in the density and the decrease in the gas sensitivity of the ZnO–Ag ceramics (Table 2).

4. Conclusion

The ZnO–Ag ceramics (0.001–3 wt% Ag_2O) sintered in air at 1170 K are suitable materials for the preparation of the ethanol resistive sensors. The grain size is 0.1–1.3 μm. The silver inclusions (clusters) are formed in the samples. The concentration of silver is higher in the bulk than at the surface probably due to the evaporation of Ag during sintering. Even at the maximum addition (3 wt%) there is

Table 2
Parameters of ZnO-based ceramics with different additives.

Additive (at%)	Sintering temperature (K)	Relative density ρ/ρ_0	Electrical conductivity (at 10 V cm^{-1}) σ_0, (Ohm^{-1} cm^{-1})	Relative dielectric permittivity ε' (at 10^5 Hz)	Coefficient of dielectric losses ε'' (at 105 Hz)	Response $(\sigma-\sigma_0)/\sigma_0$ ($P_a=26$ Pa, $T=590$ K)
–	1270	0.85	2.4×10^{-7}	443	135	1.6
0.5 Co	1270	0.85	7.9×10^{-8}	796	187	1.1
0.5 Cu	1270	0.85	3.3×10^{-11}	66	54	0.24
0.5 Ag	1270	0.7	2.2×10^{-8}	152	93	16
0.5 Ag	1170	0.6	8.9×10^{-10}	19	2	24

no the percolation across the Ag metallic phase. The electrical conduction in these materials is controlled by the grain-boundary potential barriers with the barrier height of about 0.2–0.25 eV. The response to ethanol vapor in air depends on temperature with the maximum in the range 570–600 K. In this range the sensitivity of the sensor to water vapor is negligible. At fixed temperature the response is increased with the partial pressure of ethanol according to the Freundlich isotherm. The observed increase in the response with the increase in Ag_2O addition accompanied by the decrease in the density of the ZnO–Ag ceramics, and comparison the properties of the ZnO-based ceramics with the different additives (CoO, CuO, Ag_2O) show that the role of the Ag addition can be mainly in the formation of the porous structure of zinc oxide with the high specific surface.

Acknowledgment

Authors gratefully acknowledge Ms. Nayeli Pineda Aguilar for the assistance in the microstructure characterization by SEM-EDX.

References

[1] Wang Chengxiang, Yin Longwei, Zhang Luyuan, Xiang Dong, Gao Rui, Metal oxide gas sensors: sensitivity and influencing factors, Sensors 10 (2010) 2088–2106.
[2] L.A. Obvintseva, Metal oxide semiconductor sensors for determination of reactive gas impurities in air, Russian Journal of General Chemistry 78 (12) (2008) 2545–2555.
[3] G. Korotcenkov, Metal oxides for solid-state gas sensors: what determines our choice?, Materials Science and Engineering B 139 (2007) 1–23
[4] Jong-Heun Lee, Gas sensors using hierarchical and hollow oxide nanostructures: overview, Sensors and Actuators B 140 (2009) 319–336.
[5] G. Korotcenkov, The role of morphology and crystallographic structure of metal oxides in response of conductometric-type gas sensors, Materials Science and Engineering R 61 (2008) 1–39.
[6] Chandra Sekhar Rout, S. Hari Krishna, S.R.C. Vivekchand, A. Govindaraj, C.N.R. Rao, Hydrogen and ethanol sensors based on ZnO nanorods, nanowires and nanotubes, Chemical Physics Letters 418 (2006) 586–590.
[7] Nittaya Tamaekong, Chaikarn Liewhiran, Anurat Wisitsoraat, Sukon Phanichphant, acetylene sensor based on Pt/ZnO thick films as prepared by flame spray pyrolysis, Sensors and Actuators B 152 (2011) 155–161.
[8] C. Liewhiran, S. Phanichphant, Effects of palladium loading on the response of a thick film flame-made zno gas sensor for detection of ethanol vapor, Sensors 7 (2007) 1159–1184.
[9] C. Liewhiran, S. Phanichphant, Doctor-bladed thick films of ame-made Pd/ZnO nanoparticles for ethanol sensing, Current Applied Physics 8 (2008) 336–339.
[10] Shaohong Wei, Yang Yu, Meihua Zhou, CO gas sensing of Pd-doped ZnO nanofibers synthesized by electrospinning method, Materials Letters 64 (2010) 2284–2286.
[11] N. Hongsith, C. Viriyaworasakul, P. Mangkorntong, N. Mangkorntong, S. Choopun, Ethanol sensor based on ZnO and Au-doped ZnO nanowires, Ceramics International 34 (2008) 823–826.
[12] Nguyen Le Hung, Hyojin Kim, Soon-Ku Hong, Dojin Kim, Enhancement of CO gas sensing properties in ZnO thin films deposited on self-assembled Au nanodots, Sensors and Actuators B 151 (2010) 127–132.
[13] Qun Xiang, Guifang Meng, Yuan Zhang, Jiaqiang Xu, Pengcheng Xu, Qingyi Pan, Weijun Yu, Ag nanoparticle embedded-ZnO nanorods synthesized via a photochemical method and its gas-sensing properties, Sensors and Actuators B 143 (2010) 635–640.
[14] A.Yu. Lyashkov, A.S. Tonkoshkur, V.O. Makarov, Dielectric properties of ZnO–Ag_2O gas sensitive ceramics, Photoelectronics 10 (2001) 45–46.
[15] Rui Deng, Youming Zou, Honggao Tang, Correlation between electrical, optical properties and Ag^{2+} centers of ZnO: Ag thin films, Physica B 403 (2008) 2004–2007.
[16] Chae-Seon Hong, Hyeong-Ho Park, Jooho Moon, Hyung-Ho Park, Effect of metal (Al, Ga, and In)-dopants and/or Ag-nanoparticles on the optical and electrical properties of ZnO thin films, Thin Solid Films 515 (2006) 957–960.
[17] Jin Yong Kim, Hyeong-Ho Park, A.Sivasankar Reddy, Ho Jung Chang, Hyeongtag Jeon, Youngchul Chang, Hyung-Ho Park, Electromagnetic shielder compatible ZnO transparent conducting oxides hybridized with various sizes of Ag metal nanoparticles, Ceramics International 34 (2008) 1055–1058.
[18] V.S. Khomchenko, T.G. Kryshtab, A.K. Savin, L.V. Zavyalova, N.N. Roshchina, V.E. Rodionov, O.S. Lytvyn, V.I. Kushnirenko, V.B. Khachatryan, J.A. Andraca-Adame, Fabrication and properties of ZnO:Cu and ZnO:Ag thin films, Superlattices and Microstructures 42 (2007) 94–98.
[19] Chae-Seon Hong, Hyeong-Ho Park, Seok-Joo Wang, Jooho Moon, Hyung-Ho Park, Ross H. Hill, Formation of photoresist-free patterned ZnO film containing nano-sized Ag by photochemical solution deposition, Applied Surface Science 252 (2006) 7739–7742.
[20] Li Duan, Wei Gao, Ruiqun Chen, Zhuxi Fu, Influence of post-annealing conditions on properties of ZnO:Ag films, Solid State Communications 145 (2008) 479–481.
[21] V.S. Khomchenko, V.I. Kushnirenko, V.P. Papusha, A.K. Savin, O.S. Lytvyn, Luminescent and optical properties of ZnO–Ag films, Semiconductors 44 (5) (2010) 685–690.
[22] Qun Xiang, Guifang Meng, Yuan Zhang, Jiaqiang Xu, Pengcheng Xu, Qingyi Pan, Weijun Yu, Ag nanoparticle embedded-ZnO nanorods synthesized via a photochemical method and its gas-sensing properties, Sensors and Actuators B 143 (2010) 635–640.
[23] Yong-Won Song, Kyoungwon Kim, Sang Yeol Lee, Morphology transition of Ag-doped ZnO nanostructures in hot-walled pulsed laser deposition, Thin Solid Films 518 (2009) 1318–1322.
[24] J. Jose, M. Abdul Khadar, Role of grain boundaries on the electrical properties of ZnO–Ag nanocomposites: an impedance spectroscopic study, Acta Materialia 49 (2001) 729–735.
[25] Tzung-Hsuan Lin, Tung-Te Chen, Chung-Liang Cheng, Hsia-Yu Lin, Yang-Fang Chen, Selectively enhanced band gap emission in ZnO/Ag2O nanocomposites, Optics Express 17 (6) (2009) 4342–4347.
[26] Litty Irimpan, V.P.N. Nampoori, P. Radhakrishnan, Spectral and nonlinear optical characteristics of nanocomposites of ZnO–Ag, Chemical Physics Letters 455 (2008) 265–269.
[27] Shu-Ting Kuo, Wei-Hsing Tuan, Jay Shieh, Sea-Fue Wang, Effect of Ag on the microstructure and electrical properties of ZnO, Journal of the European Ceramic Society 27 (2007) 4521–4527.
[28] Zhi-Peng Sun, Lang Liu, Li Zhang, Dian-Zeng Jia, Rapid synthesis of ZnO nano-rods by one-step, room-temperature, solid-state reaction and their gas-sensing properties, Nanotechnology 17 (2006) 2266–2270.
[29] Doerffel Klaus, Statistik in der analytischen Chemie, Dt. Verl. für Grundstoffindustrie, 1987, 192s.
[30] Ya. E. Geguzin, Sintering Physics, Nauka, Moscow, 1984, 312p (in Russian).
[31] F. Kremer, A. Schonhals, W. Luck, Broadband Dielectric Spectroscopy, Springer Verlag, New York, 2002.
[32] T.K. Gupta, Application of zinc oxide varistors, Journal of American Ceramic Society 73 (7) (1990) 1817–1840.

[33] M. Green, Solid State Surface Science, New York, 1969.
[34] A.N. Gruzintsev, V.T. Volkov, E.E. Yakimov, Photoelectric properties of ZnO films doped with Cu and Ag acceptor impurities, Semiconductors 37 (3) (2003) 259–262.
[35] Sheng-Po Chang, Shoou-Jinn Chang, Chien-Yuan Lu, Meng-Ju Li, Cheng-Liang Hsu, Yu-Zung Chiou, Ting-Jen Hsueh, I-Cherng Chen, A ZnO nanowire-based humidity sensor, Superlattices and Microstructures 47 (2010) 772–778.
[36] A.B. Glot, Effect of humidity on the conductivity of ZnO–TiO_2 ceramics doped with MnO_2 and La_2O_3, Inorganic Materials 33 (8) (1997) 832–834.
[37] L.Yu. Kupriyanov, Semiconductor sensors in physico-chemical studies, Handbook of Sensors and Actuators, vol. 4, Elsevier Science B. V, Amsterdam, 1996, p. 18.
[38] A. Pandey, A. Prasad, S. Singh, O. Parkash, D. Kumar, Effect of manganese and cobalt doping on conductivity of ZnO based varistors: a study by complex plane modulus, Journal of Materials Science: Materials in Electronics 19 (11) (2008) 1122–1127.
[39] F.F. Volkenstein, The Electronic Theory of Catalysis on Semiconductors, Pergamon, New York, 1963.
[40] A.Yu. Lyashkov, A.S. Tonkoshkur, V.O. Makarov, Gas sensing properties of WO_3-based ceramics to ethanol vapors, Sensors and Actuators B 148 (2010) 1–5.